

Trajectory Analysis of Liquid Fuel Injected Normally to High-Enthalpy Supersonic Crossflows

Justin Sprunger, Nathan Dreyer, Kareem Ahmed
Department of Mechanical and Aerospace Engineering, University of Central Florida
Orlando, Florida, United States

1 Abstract

Liquid fuel jets were injected perpendicular to a high enthalpy supersonic free stream. The fuel used was Jet-A, and the free stream was generated from an H₂-Air, vitiated Mach 4.5 wind tunnel. High-speed schlieren photography was employed to qualitatively and quantitatively study the jet's primary breakup mechanism and free stream penetration height, respectively. Through multiple test campaigns the injector diameter and momentum flux ratio were varied. Previous works have conducted liquid jet into supersonic crossflow (LJISC) experiments; however, few groups have simultaneously experimented with fuel at flight relevant enthalpies. The data taken in the current study is compared to that of previous works. It is shown that although large differences in Mach number, stagnation properties, and jet compositions are used, trajectory results resemble a similar trend.

2 Introduction

LJISC's have been explored in relation to high speed airbreathing propulsion for the previous six decades. Early work investigated the effects of injector configurations and free stream conditions on the jet's trajectory. Through this work, an experimentally derived power fit correlation was introduced to visualize the steady state trajectory coordinates. Since then, most studies have followed suit and represented data in a similar manner. A summary of these correlations from relevant studies and their respective facility conditions can be seen in table 1. Although the empirically derived trajectory formulas are a useful tool for comparing data sets, the information regarding the dominating physics is not included. Additionally, differences in experimental techniques used to determine the jet boundary can lead to different results, as demonstrated by K.C. Lin et al [1] in the comparison between two different boundary definition techniques. To aid in the creation of a physics-based trajectory formulation the comparison of the current works data to those at different boundary conditions is made. To fully understand the implications of this comparison, the previous experiments methodologies will be quickly reviewed in this section.

Table 1: Previous experimental conditions and trajectory curves

<i>Author</i>	<i>P₀ (psi)</i>	<i>T₀ (K)</i>	<i>Mach</i>	<i>D_{inj} (in)</i>	<i>J</i>	<i>Fluid</i>	<i>Correlation</i>
Kush & Schetz	40 – 140	300	2.4 & 4	1/32" & 1/16"	1.2 – 18	Water, Glycol/Water	$\left(\frac{y}{d_{inj}}\right)_{Max} = 6 * (J^{0.49})$
Perurena et al.	290	510	6	0.039"	2 – 10	Water	$\left(\frac{y}{d_{inj}}\right) = 3.5 * (J^{0.3}) * \left(\frac{x}{d_{inj}}\right)^{0.38}$
Lin et al.	30	530	1.94	0.039" & 0.020"	2-15	Water	$\left(\frac{y}{d_{inj}}\right) = 4.73 * (J^{0.3}) * \left(\frac{x}{d_{inj}}\right)^{0.3}$
Sathiyamoorthy et all	58	1562	2	0.039"	10,15,23	Kerosene	$\left(\frac{y}{d_{inj}}\right) = 3.94 * (J^{0.47}) * \left(\frac{x}{d_{inj}}\right)^{0.3}$
Catton et al	250 - 710	300	4.1	0.025" & 0.035"	7 – 178	Water, Freon, DC-2, & Methanol	$\left(\frac{y}{d_{inj}}\right) = 3.8 * (J^{0.39}) * \left(\frac{x}{d_{inj}}\right)^{0.23}$ <i>See reference</i>

First, considering a hypersonic free stream case, Perurena et al [2] conducted experiments in a Mach 6 pebble bed heated blow down wind tunnel with stagnation conditions of 500K. Measurements of penetration were made with schlieren imaging. The boundary was determined through averaging images and taking a threshold of standard deviation to be the jet boundary. Although the value is not stated, it can be qualitatively observed through the PDF plots. Lin et al performed experiments in a vitiated 1.94 Mach number wind tunnel with stagnation temperatures of about 500K. Details of the wind tunnel can be found in [3]. Lin injected multiple liquids and found the jet boundary using both phase Doppler particle analyzer (PDPA) and schlieren imaging. Results of both were used. Catton et al [4] used a Mach 4.1 wind tunnel with near ambient total temperatures and total pressures between 250 and 710 psi. They injected multiple liquids at a range of angles and injection pressures. Boundaries were determined with line-of-sight imaging. Catton also compared the observed liquid boundary with previous studies up to Mach 8 and found good agreement with both experimental and numerical data.

3 Experimental Setup & Methodology

The experiments were carried out in the HyperReact wind tunnel at the University of Central Florida. A diagram of the hardware is shown in figure 1. In short, HyperReact is a H₂-Air vitiated blow down wind tunnel with configurable CD nozzles. The Nozzle used for this study has an area ratio of 25, leading to an operation Mach number of about 4.5 at nominal temperature. Directly downstream of the CD nozzle is the modular injection plate. 5 diameters were tested ranging from 0.007 to 0.040 inches. Details of the injectors tested are displayed in table 2. Flow rate checks were performed, and the respective discharge coefficients were used when calculating the jet velocity. In the preburner, a K-type thermocouple and CTAP pressure transducer were used to determine stagnation temperature and pressure respectively. A transducer in the fuel manifold directly upstream of the injector was used to measure fuel injection pressure. A piston accumulator was used to pressurize the fuel up to 1100 psi. Schlieren and shadowgraph photography were performed at 40k fps with a shutter speed of 160ns.

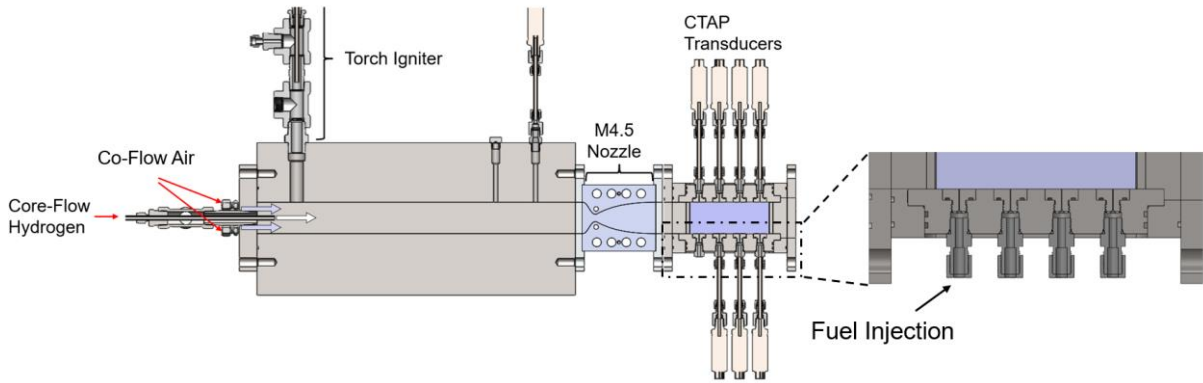


Figure 1: HyperReact facility with extended view of modular injection plate

Using a chemical kinetics solver, the vitiated gas properties are found. With the CD nozzle area ratio, and preburner temperature and pressure measurements, the Mach number exiting the CD nozzle is found. With the isentropic relations, the expanded fluid properties are calculated. This method is verified by comparing a pressure trace directly after the nozzle and recording very good agreeance. Through this process the momentum flux of air is calculated. Using the injection pressure measurement and the previously measured discharge coefficient, the velocity of the jet was calculated. The density of the fuel was also measured to be 785 kg/m^3 . With these values the momentum flux ratio (J) was found.

Table 2: Crossflow and liquid jet conditions for all injector diameters tested

D_{inj}	T_0 (K)	P_0 (psi)	M_{TS}	γ_{PB}	T_{TS} (K)	P_{TS} (psi)	V_{TS} (m/s)	V_{fuel} (m/s)	J
0.007"	1090	1242	4.51	1.32	257	3.13	1443	66	5.92
	1115	1250	4.50	1.32	266	3.17	1463	98	12.92
	1066	1254	4.52	1.32	250	3.14	1426	117	18.28
	1086	1253	4.51	1.32	256	3.15	1441	134	23.90
0.010"	1081	1261	4.52	1.32	254	3.16	1437	49	3.16
	1066	1250	4.52	1.32	249	3.12	1424	74	7.28
	1089	1251	4.51	1.32	257	3.15	1443	87	10.04
	1082	1256	4.52	1.32	254	3.15	1437	101	13.66
0.016"	1065	1243	4.52	1.32	249	3.10	1423	49	3.23
	1085	1254	4.51	1.32	256	3.15	1440	74	7.36
	1067	1241	4.52	1.32	250	3.11	1426	82	9.18
	1058	1237	4.53	1.32	246	3.08	1418	104	14.57
0.025"	1091	1186	4.51	1.32	258	2.98	1444	39	2.13
	1047	1189	4.53	1.32	243	2.95	1410	64	5.77
	1047	1183	4.53	1.32	243	2.94	1410	89	11.32
	1043	1180	4.53	1.32	242	2.93	1407	111	17.63
0.040"	1459	1198	3.96	1.29	443	6.12	1669	39	1.41
	1413	1194	3.98	1.29	424	6.05	1637	57	2.98
	1431	1198	3.97	1.29	431	6.09	1650	69	4.29
	1395	1187	3.98	1.30	417	5.99	1625	80	5.97
	1405	1194	3.98	1.29	421	6.04	1632	89	7.18
	917	1206	4.60	1.33	203	2.87	1306	41	2.34
	860	1190	4.64	1.34	185	2.77	1259	64	5.75
	1002	1226	4.55	1.32	230	3.01	1375	72	7.15
	1012	1209	4.55	1.32	233	2.98	1383	80	8.90
	1400	1135	4.39	1.30	363	3.09	1673	30	1.30
	1484	1129	4.36	1.29	395	3.13	1733	45	2.98
1397	1084	4.39	1.30	363	2.95	1671	57	5.06	

To perform the trajectory analysis, 5000 images were used from each run, resulting in a total time of 125ms. The frames were normalized by the maximum pixel intensity, averaged, and the standard deviation was taken through time. Because the average image intensity more closely represents the dense jet plume, the average images were used to determine a boundary pixel intensity. A pixel intensity of 80% was taken as the plume edge. The process shown in figure 3 outlines the image processing steps for this data set. The frames were normalized, binarized with the 80% criteria, and the contour was traced using an image processing software. With the pixel coordinates and the spatial calibration, the trajectories were normalized by injector diameter.

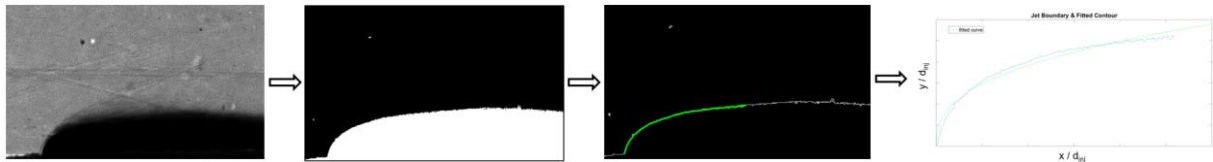


Figure 2: Boundary tracing process

4 Results and Discussion

Internal Trajectory Analysis 4.1

The results from the runs listed in table 2 are shown in figure 4. Due to the maximum penetration occurring within one to two inches downstream of the injector, the focus for the comparison was maximum penetration. For flight relevant geometries, where functional combustor geometries would be located significantly downstream, trajectory in the near region of the jet is most likely non-critical and would not be a design factor. Therefore, the maximum penetration heights were analyzed in this data set. When nondimensionalizing the trajectories by injector diameter, two groups can be seen.

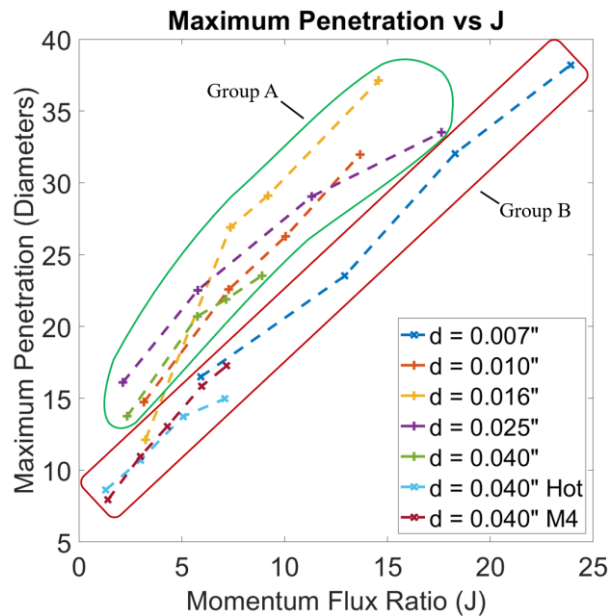


Figure 3: Maximum penetration achieved for range of injector diameters through all J's tested

For the injectors tested at lower stagnation temperatures (860K – 1115K, excluding $d_{inj} = 0.007''$) The data points can be represented by trend A. Analyzing the individual injector sets, it can be seen that from runs 1-2 the initial slope is higher than those of 2-4 (Lowest to highest J). For some cases, the slope evens out after the initial J value. This matches observations by Schetz [5] who recorded 3 different modes for a similar J range. For all cases in group A, the slope decreases as J is increased. This result is

intuitive, as the jet velocity and consequentially, free stream penetration is increased, the jet becomes increasingly unstable. Although the extra momentum is beneficial for a cohesive jet, the increased mass loss from the added breakup has a counteractive affect. Group B consists of injectors tested at high stagnation temperatures (1395K – 1485K) as well as the 0.007 inch injector. For this group, a higher J value is needed to obtain a similar penetration as group A. Additionally, the linearity of this trend occurs over a range of injector diameter, Mach number, and stagnation temperature. It is of interest to note that these three cases involve the high temperature conditions and the smallest diameter only. It is possible that the higher temperature reduces the penetration dependence to fewer parameters. (For the observed range). If the effect can be isolated, the results would offer insight into the overall controlling factors for a transverse jets trajectory.

External Trajectory Analysis 4.2

Comparing the empirically derived jet trajectories to multiple experimental works (Figure 4). It can be observed that even through the variation of Mach number, jet diameter, selected fluid, and temperature, the predicted trajectories from the empirical correlations fall within the standard deviation of the jet wake. Due to the differences in methodology of defining the jet boundary, some variation of trajectories is expected. The high standard deviation outlines the area where the primary breakup is occurring, leading to low intensities for the averaged image approach. PDPA based correlations will indicate the outermost reach of droplets/liquid, covering the initial gradient of the standard deviation as it transitions to the free stream. These correlations aligning with the outer edge of the standard deviation image indicate that there is good agreeance between the predicted correlations and the current works experimental data.

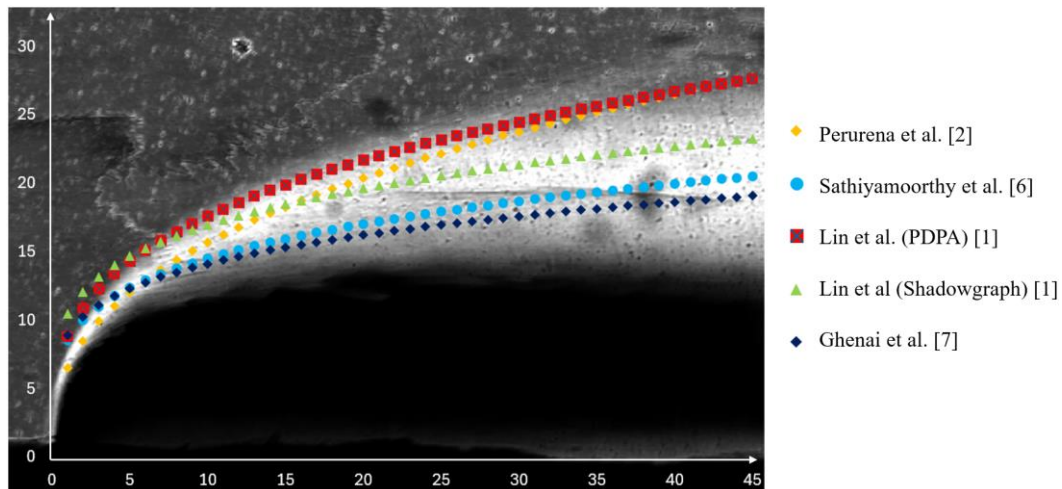


Figure 4: Transverse jet trajectories for previous experiments plotted over standard deviation scene

5 Conclusion

Liquid jets of kerosene-based fuels were injected into a supersonic free stream at flight relevant enthalpies. The jet wake was recorded with high-speed schlieren, and boundaries were defined through intensity values of averaged images. Upon nondimensionalizing the free stream penetration by injector diameter, two distinct groups can be seen. The minor group encompasses the tests performed at a higher temperature, along with the smallest diameter tested at the lower temperature. Compared to the majority, the minor group maintains a linear trend, although further testing is needed to ensure the linearity will be maintained for the higher J values. When reviewing results from literature, methods for determining jet boundary impact comparisons, however it is evident the current works results align with previous work, as the maximum and minimum boundary definitions through all groups fall within spatial standard deviation of the observed jet wake. Considering the boundary condition variations between all sources,

the significance of the momentum flux ratio and the weak dependence of static properties of the free stream is highlighted.

References

- [1] Lin K-C, Kennedy P.J., Jackson T.A. (2002) Penetration heights of liquid jets in high-speed crossflows. *40th AIAA Aerospace Sciences Meeting & Exhibit*, AIAA-2002-0873.
- [2] Perurena J.B., Asma C.O., Theunissen R., Chazot O. (2009) Experimental investigation of liquid jet injection into Mach 6 hypersonic crossflow. *Experiments in Fluids*, 46:403-417. <https://doi.org/10.1007/s00348-008-0566-5>.
- [3] Gruber M.R., Baurle R.A., Mathur T., Hsu K-Y. (2001) Fundamental studies of cavity-based flameholder concepts for supersonic combustors. *Journal of Propulsion and Power*, 17(1):146-153.
- [4] Catton I., Hill D.E., R.P. (1968) Study of liquid jet penetration in a hypersonic stream. *AIAA Journal*, 6(11):2084-2089.
- [5] Schetz J.A., Kush E.A. Jr., Joshi P.B. (1980) Wave phenomena in liquid jet breakup in a supersonic crossflow. *AIAA Journal*, 18(7):774-781.
- [6] Ghenai C., Sapmaz H., Lin C-X. (2009) Penetration height correlations for non-aerated and aerated transverse liquid jets in supersonic cross flow. *Experiments in Fluids*, 46(1):121-129. <https://doi.org/10.1007/s00348-008-0547-8>.
- [7] Sathiyamoorthy K., Danish T.H., Iyengar V.S., Srinivas J., Harikrishna X., Muruganandam T.M., Chakravarthy S.R. (2020) Penetration and combustion studies of tandem liquid jets in supersonic crossflow. *Journal of Propulsion and Power*, 36(6):920-930. <https://doi.org/10.2514/1.B38047>.
- [8] Fdida N., Mallart-Martinez N., Le Pichon T., Vincent-Randonnier A. (2022) Penetration of a kerosene liquid jet injected in a high-temperature Mach 2 supersonic crossflow. *Experiments in Fluids*, 63(10):154. <https://doi.org/10.1007/s00348-022-03480-z>.
- [9] Su Y-H., Yuan H.F., Su Y-P. (2020) Liquid-fuel injection into supersonic cross flow. *Combustion Science and Technology*. <https://doi.org/10.1080/00102202.2020.1758683>.